JAAS

ROYAL SOCIETY OF CHEMISTRY

PAPER

View Article Online
View Journal | View Issue

Cite this: J. Anal. At. Spectrom., 2025, 40, 2038

LIBS quantitative analysis based on multi-model calibration marked with characteristic lines

Baining Xu, [a] Zhongqi Hao, *[a] Yuanhang Wang, [b] Li Liu,[a] Neng Zhang,[a] Yu Rao,[a] Lei Wang,[a] Jiulin Shi*[a] and Xingdao He[a]

Received 10th April 2025
Accepted 2nd June 2025

DOI: 10.1039/d5ja00132c

rsc.li/jaas

Long-term reproducibility remains one of the important challenges in laser-induced breakdown spectroscopy (LIBS) quantitative analysis. In this work, a novel LIBS quantitative method based on multi-model calibration marked with characteristic lines was proposed. Under identical experimental equipment and parameters, multiple calibration models were established by using LIBS data collected at different time intervals. Simultaneously, the characteristic line information, which reflects variations in experimental conditions, was marked as the characteristic of each calibration model. During the analysis of unknown samples, the optimal calibration model was selected for quantitative analysis by characteristic matching. Taking the analysis of Mo, V, Mn, and Cr elements in alloy steel as an example, ten calibration models were established based on daily spectral data, and the test samples were quantitatively validated for five days. The results indicate that, compared to the single calibration model, the calibration model selected through the matching of characteristic lines significantly improves the average relative errors (ARE) and the average standard deviations (ASD). The method proposed in this study provides a new quantitative analysis idea for LIBS technology, which can effectively improve the reproducibility of LIBS long-term repeated measurements.

1. Introduction

Laser-induced breakdown spectroscopy (LIBS) is an atomic emission spectroscopy technique that employs high-energy focused laser pulses to generate plasma from samples.[1] The LIBS technique offers distinct advantages over traditional chemical analysis methods, including minimal invasiveness, rapid analysis, simple sample preparation, simultaneous detection of multiple elements, and *in situ* detection.[2,3] Therefore, LIBS has been widely applied in various fields, such as the metallurgical industry,[4] coal industry,[5] environmental monitoring,[6] space exploration,[7,8] biological application,[9] and food safety.[10] However, due to the influence of laser energy fluctuation, equipment parameter drift, environmental conditions change, human operation error and other factors, the calibration model of LIBS quantitative analysis has difficulty remaining effective in the long term, that is, the error of the quantitative results obtained using the established calibration model increases as time progresses.[11–15] To ensure the measurement accuracy, it is often necessary to re-establish the calibration model before measurement, but this significantly undermines the advantages of LIBS rapid detection and hinders its commercialization and instrumentation development.[16,17] Therefore, it is of great significance to study methods to improve the long-term reproducibility of LIBS quantitative analysis.

In recent years, researchers have made various efforts to reduce LIBS spectral fluctuation and enhance the reproducibility of detection results. For instance, in 1998, Panne *et al.* first proposed standardizing the spectral intensity by plasma characteristics (such as electron temperature and electron number density) to cope with the influence of experimental conditions on the calibration model. This method significantly improves the short-term stability of LIBS analysis by dynamically adjusting the spectral response through real-time diagnosis of plasma parameters and lays a foundation for the wide application of the subsequent internal standard method. However, for a single calibration model, this method is prone to failure due to long-term equipment parameter drift or cumulative environmental changes and cannot cope with long-term measurement.[18] Feng *et al.* proposed a spectral normalization method based on plasma characteristics, which uses plasma characteristic parameters to correct the original spectral data. This method compensates for the fluctuation of characteristic line intensity caused by the change of plasma temperature, ionization degree and total particle number density of the measured elements, and the method effectively reduced the uncertainty of spectral intensity and improved the accuracy of LIBS quantitative analysis.[19] Hao *et al.* introduced the two-point

[a]Jiangxi Provincial Key Laboratory of Optoelectronic Information Perception Technology and Instruments, Nanchang Hangkong University, Nanchang, 330063, China. E-mail: hzq@nchu.edu.cn; jlshi@nchu.edu.cn

[b]Department of Nuclear Physics, China Institute of Atomic Energy, Beijing, 102413, China

standardization (TPS) method, which effectively corrected instrumental drift, significantly reducing the average relative error (ARE) for various elements and improving the long-term reproducibility of LIBS quantitative analysis. However, the correction results of this method depend on the selection of reference samples.[20] Hou *et al.* converted the Gaussian beam into a dome beam, resulting in a more uniform and stable plasma, thereby enhancing the intensity and stability of LIBS spectral signals.[21] Liu *et al.* employed partial least squares regression (PLSR) to establish a relationship model between the relative deviation of the laser pulse energy distribution and the LIBS spectral intensity, and used the pulse energy distribution to correct the spectral intensity. As a result, the long-term relative standard deviation of copper and silicon samples decreased from 13.5% and 10.7% to 4% and 6.5%, respectively, and the long-term repeatability of LIBS measurement was significantly improved.[22] Xu *et al.* calibrated the element quantitative analysis model based on the correlation between the plasma acoustic signals and the spectral signal. Using the acoustically corrected model, the average relative standard deviation (ARSD) of the spectral intensity for Cr, Mo, Ni and V elements was reduced by 26.7%. The ARE of 48 hours decreased by 38.6%, and the spectral ARSD of 8 days was significantly reduced by 43.1%, thereby achieving notable improvements in the long-term repeatability of LIBS quantitative analysis.[23] Nie *et al.* proposed a spectral standardization method based on plasma image-spectrum fusion (SS-PISF) to correct for the parameter changes of plasma. Through experimental verification on aluminum alloy, alloy steel and ore briquetting samples, it is proved that the SS-PISF method can significantly improve the determination coefficient (R^2) of the calibration curve, reduce the standard deviation and improve the LIBS spectral stability compared with the full spectral normalization method and the simplified spectral normalization method.[24] Lu *et al.* proposed a Kalman filtering algorithm to calibrate the calibration model, which can improve the long-term reproducibility of LIBS quantitative analysis.[25] Just recently, Zhang *et al.* proposed an artificial neural network calibration method based on multi-period data fusion. By integrating spectral data of different time periods and combining the back propagation neural network model optimized by genetic algorithm, the accuracy and stability of LIBS long-term repeated measurement results are significantly improved.[26]

In summary, laser-induced plasma contains a wealth of important information, such as LIBS spectral information, acoustic signals, and plasma images, which can be utilized for the establishment and calibration of calibration models to improve the accuracy and stability of LIBS quantitative analysis. Although the multi-dimensional information contained in the laser-induced plasma provides a potential direction for the optimization of the calibration model, its practical application needs to consider the detection efficiency and data reliability. As the core output of the LIBS system, spectral information has real-time characteristics and convenient data acquisition. Among them, the selection of matrix element characteristic line information as a marker has significant advantages. Because the content of matrix elements is stable, such as iron, which accounts for a stable proportion (>90%) in alloy steel samples, and the content changes little in different samples, the change in characteristic line intensity is mainly due to the drift of experimental conditions (such as laser energy fluctuation, environmental temperature, and humidity change), rather than the difference in sample composition. In addition, most of the existing studies use a single calibration model for quantitative analysis, but this type of model has significant limitations: due to its sensitivity to changes in experimental conditions, it leads to a decline in analytical performance in long-term measurements. The specific performance issue is that the prediction results deviate from the true value, and the stability is poor. To address this issue, this study proposes a LIBS quantitative analysis method based on multi-model calibration marked with characteristic lines, aiming to improve the long-term reproducibility of LIBS quantitative analysis.

2. Experimental

2.1 Experimental setup

Fig. 1 illustrates the schematic diagram of the LIBS experimental system. A Q-switched Nd: YAG pulsed laser (Continuum Precision-II, wavelength 532 nm, frequency 10 Hz, and pulse width 10 ns) serves as the plasma excitation source. The laser beam is divided by a beam splitter into transmitted and reflected beams at a ratio of 5 : 95. The transmitted beam is directed to a photodetector (Thorlabs-DET25K, wavelength range 150–550 nm, rise time 55 ns, active area 4.8 mm^2), which converts the laser pulse into an electrical signal used as a synchronous trigger for the spectrometer. The reflected beam is focused on the surface of the sample using a focusing lens (f = 150 mm). To avoid plasma shielding caused by air breakdown, the focal point of the lens is positioned 4 mm below the sample surface. The sample is placed on a three-dimensional electric displacement platform and moves horizontally with the displacement platform, so that each laser pulse can act on a new position on the surface of the sample, thereby preventing the laser from repeatedly ablating the same position on the surface of the sample. The emission spectrum of the plasma is collected by a paraxial light collector and coupled into an

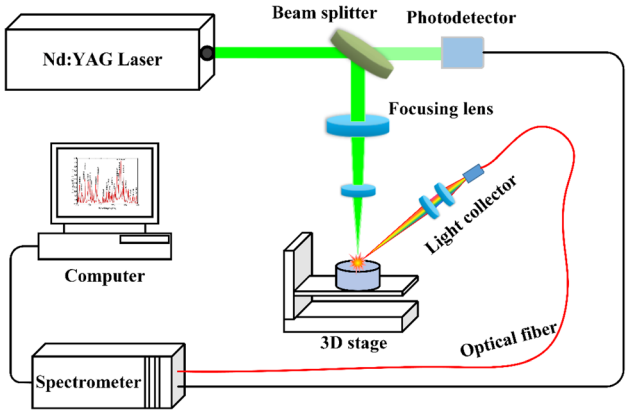

Fig. 1 Schematic diagram of the LIBS experimental system.

optical fiber. The optical signal is then transmitted through the fiber to the spectrometer (AvaSpec-ULS4096CL-3EVO, wavelength range 200–485 nm, spectral resolution 0.05 nm).

The LIBS experimental parameters were optimized based on the signal-to-noise ratio (SNR), with the optimal conditions determined as follows: laser pulse energy of 60 mJ, spectral acquisition delay of 2 μs, and defocus amount of −4 mm (the distance from the laser focal point to the sample surface).[27,28] During data acquisition, each sample collected 5 spectra, with each spectrum representing the average of 10 laser pulses, respectively, for the modeling samples to collect 10 days of spectral data and for the test samples to collect 5 days of data. All data were processed using the program written in Matlab™ R2016a.

2.2 Experimental sample

The experimental samples were all national standard samples of alloy steel. The samples were polished and cleaned before the experiment to ensure the consistency of the surface and reduce the influence of the surface characteristics of the samples on the experimental results. The composition and number are shown in Table 1. Based on the high, medium, and low levels of elemental content, two samples were selected from each type of steel. Specifically, samples 5, 6, 9, 11, 16 and 18 were chosen as test samples (marked with *) for validation, while the remaining samples were used as modeling samples to establish the calibration model.

3. Method

3.1 Multi-model calibration marked with characteristic lines

Fig. 2 shows the flow diagram of the LIBS quantitative analysis method based on multi-model calibration marked with characteristic lines. The meaning of each symbol in the flow diagram is as follows: $I_t(j)$ represents the characteristic line intensity of the j-th test sample under the current experimental conditions, and its value directly reflects the current real-time experimental state. $I_c(i)$ denotes the mean intensity of the characteristic line for the modeling sample corresponding to the i-th calibration model, which represents the reference value for historical experimental conditions. $M_E(i)$ is defined as the distance between the i-th calibration model and the characteristic line value of the current test sample (that is, the Euclidean distance between $I_t(j)$ and $I_c(i)$), which is used to represent the proximity of the experimental conditions. Under identical experimental equipment and parameters, multiple calibration models were established by using LIBS data collected at different time intervals. Simultaneously, the characteristic line information, which reflects variations in experimental conditions, was marked as the characteristic of each calibration model. During the analysis of unknown samples, the optimal calibration model was selected for quantitative analysis by characteristic matching. This method assesses the consistency of experimental conditions by the similarity of the characteristic lines and identifies the model with the smallest deviation of the characteristic line. Since the experimental conditions under which the model is established are closest to those of the current test samples, this approach effectively mitigates the impact of temporal and environmental changes on the LIBS signal, thereby enhancing the accuracy and long-term reproducibility of LIBS quantitative analysis. Moreover, by developing a multi-period calibration model mechanism for the dynamic matching of characteristic lines, the frequent demand for re-establishing the calibration model is effectively avoided.

3.1.1 Selection of analytical spectral lines. The basic calibration method is a quantitative analytical approach that establishes a model based on the correlation between the

Table 1 Composition of Mn, Cr, Mo, and V elements from the alloy steel samples (wt%)

Sample no.	Manufacturers	National standard sample number	Mn	Cr	Mo	V
1	Shenyang Institute of standard samples, China	GSB 03-1525-2002/1	0.503	2.460	0.600	0.140
2		GSB 03-1525-2002/2	0.243	0.860	0.290	0.628
3		GSB 03-1525-2002/3	0.930	1.430	0.109	0.074
4		GSB 03-1525-2002/4	1.330	0.278	0.404	0.031
5*		GSB 03-1525-2002/5	2.100	1.830	0.860	0.900
6*		GSB 03-1525-2002/6	1.320	3.160	1.000	0.355
7	NCS testing technology CO., LTD, China	GBW(E) 010515	0.414	0.212	0.157	0.010
8		GBW(E) 010516	0.646	0.127	0.208	0.062
9*		GBW(E) 010517	1.960	0.640	0.306	0.149
10		GBW(E) 010518	0.176	0.098	0.071	0.215
11*		GBW(E) 010519	1.640	0.436	0.257	0.105
12		GBW(E) 010520	1.050	0.374	0.104	0.042
13		GBW(E) 010521	0.117	0.077	0.029	0.326
14	Central iron & steel research Institute, China	GBW 01666a	0.680	2.970	0.210	0.189
15		GBW 01667a	3.600	0.950	0.019	0.478
16*		GBW 01668a	0.890	2.270	0.556	0.346
17		GBW 01669a	2.420	4.400	1.400	0.449
18*		GBW 01670a	1.040	1.360	0.864	0.118
19		GBW 01671a	1.880	3.270	0.118	0.273
20		GBW 01672a	0.325	0.703	0.305	0.013
21		GBW 01673a	0.553	0.177	0.423	0.055

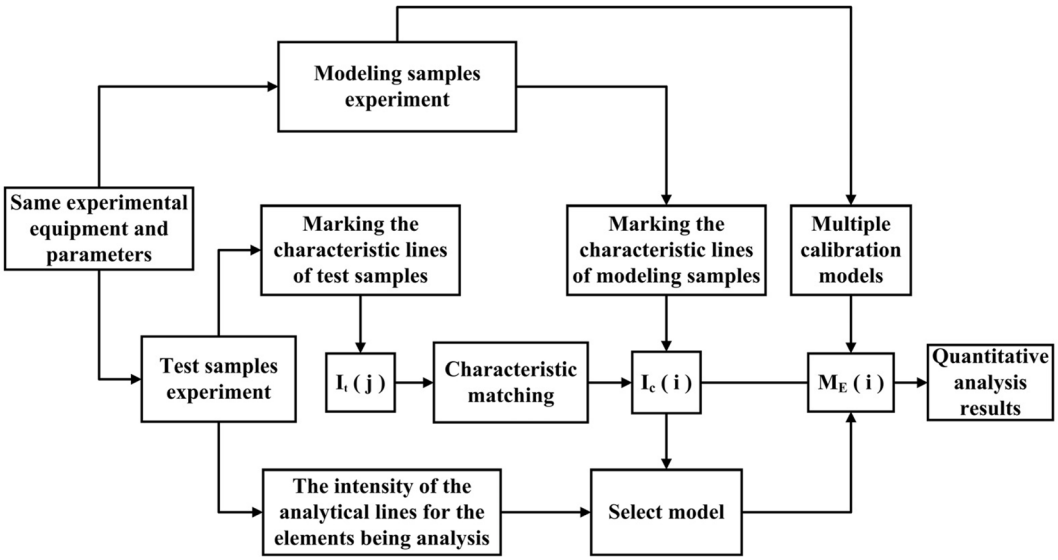

Fig. 2 Flow diagram of the LIBS quantitative analysis method based on multi-model calibration marked with characteristic lines.

intensity of spectral lines and the concentration of elements. This method is widely recognized as the most employed, physically significant, and representative quantitative analysis model in LIBS.[29,30] In the present study, alloy steel samples were analyzed for four elements: Mo, V, Mn, and Cr. To identify the optimal analytical lines for these elements, LIBS experimental equipment was utilized to systematically collect the spectral intensity data of the 15 modeling samples listed in Table 1. According to the NIST atomic spectrum database and the spectra collected by the experiment, the spectral lines with high signal intensity, small background interference, and no peak interference or overlapping peaks in each element were selected for analysis. Then, the linear relationship model between the intensity of each spectral line and the concentration of the corresponding element was established based on the basic calibration method. By comparing the determination coefficients (R^2) of various spectral lines, those with higher R^2 values were chosen as the analytical spectral lines. As illustrated in Fig. 3, the spectral lines Mo II 281.62 nm, V I 437.92 nm, Mn I 478.34 nm, and Cr II 286.51 nm were ultimately selected for modeling the four elements. The determination coefficients (R^2) for the basic calibration models of these spectral lines were 0.990, 0.985, 0.995, and 0.991, respectively, indicating a strong linear relationship between the concentration of each element and the corresponding spectral intensity.

3.1.2 Development of multiple calibration models. Fig. 4 presents ten calibration models for each of the four elements Mo, V, Mn, and Cr, which were developed by collecting LIBS spectra under identical experimental equipment and parameters. The spectra were collected at 24 hour intervals over ten days. Utilizing the chosen analytical spectral lines in conjunction with the 10 days spectral dataset, the basic calibration method is employed to develop a daily calibration model. As shown in Fig. 4, the ten-day calibration models of the four elements all showed high determination coefficients, ranging from 0.937 to 0.998, which indicated that the calibration models of each day could still maintain a good linear relationship with the change of time. However, through observation, it can be found that the calibration models of different days had significant differences in slope and intercept. This is because each calibration model contains information on the experimental conditions of the day, such as laser energy fluctuation, equipment parameter drift, human operation error, environmental condition change, and other unpredictable factors.[26,31] The cumulative effect of these variables is reflected in the alterations of the slope and intercept of the calibration curves. Because the change of these factors is random, the slope and intercept of the calibration curve will not increase or decrease monotonously. However, when the experimental device and parameter settings remain unchanged, the changes of these factors can only be in a limited range. Although the 10 days calibration curve shown in Fig. 4 cannot include all the changes, it can still reflect the range of changes to a certain extent. This study aims to demonstrate the feasibility of enhancing the long-term reproducibility of LIBS quantitative analysis using a method based on multi-model calibration marked with characteristic lines with 10 days analysis data.

3.1.3 Marking of characteristic lines. To find information that can accurately reflect the changes in experimental conditions and achieve the matching of the optimal calibration model, the marking of characteristics is particularly important. As the main information component of the whole LIBS spectrum, the spectral lines are the primary characteristic marker. In the analysis of alloy steel samples, the matrix element iron (Fe) is the main element in the alloy steel sample, and its content usually accounts for more than 90% of the total sample, with little variation in different samples. This stability means that the change in the characteristic line intensity of Fe mainly arises from changes in experimental conditions, rather than from composition differences of the sample itself. Therefore, it

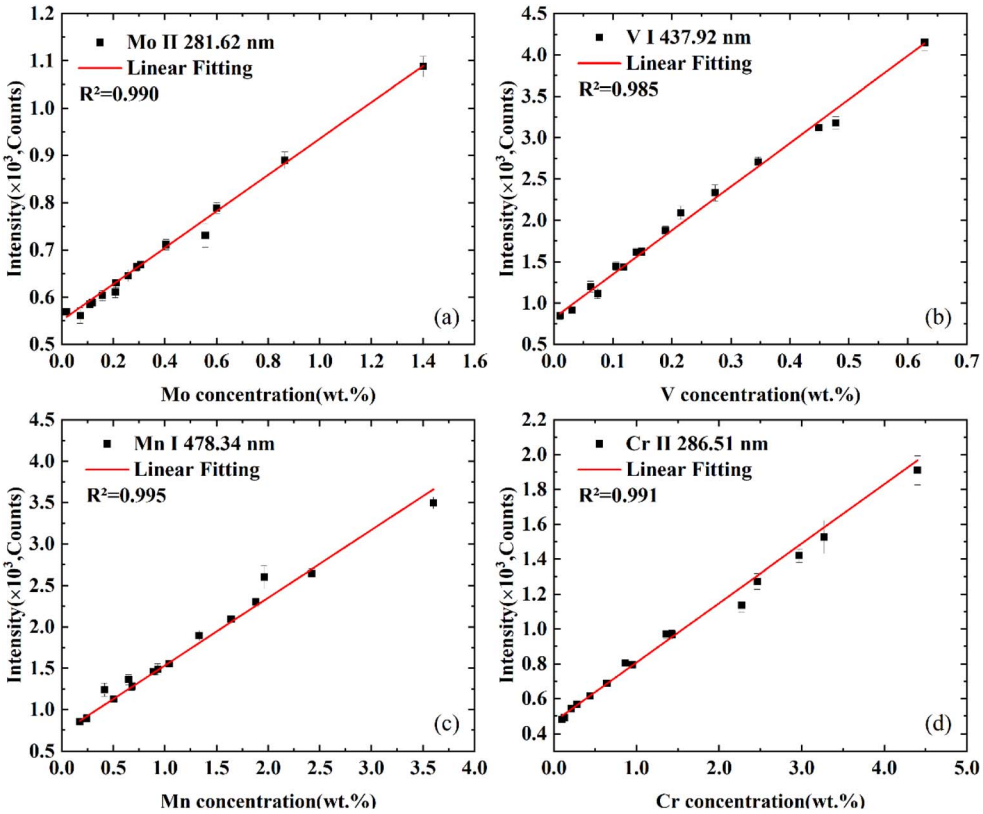

Fig. 3 Calibration model of the analytical spectral lines: (a) Mo II 281.62 nm; (b) V I 437.92 nm; (c) Mn I 478.34 nm; (d) Cr II 286.51 nm.

is feasible to mark the characteristic line of Fe as characteristic to reflect the change in experimental conditions. To ensure the applicability of the characteristic lines, the selection of the characteristic lines should refer to the following criteria: (1) to avoid the influence of the self-absorption effect, the weak lines of the Fe element should be selected; (2) the selected lines should be free from overlaps or interference from other peaks; (3) the selected lines should be clearly distinguishable within the resolution range of the spectrometer.

3.1.4 The matching method of characteristic lines. In the LIBS quantitative analysis based on multi-model calibration marked with the characteristic lines, the Euclidean Distance method is used to match the characteristic lines. This method is commonly used to calculate the straight-line distance between two points in multi-dimensional space. In this study, it was employed to calculate the distance between the characteristic line values of the test samples on verification days and the characteristic line values of calibration models from different time periods. The calibration model with the shortest distance was then selected for quantitative analysis. The calculation formula for Euclidean Distance is as follows:

$$d = \sqrt{\sum_{i=1}^{n} (x_i - y_i)^2} \quad (1)$$

where x_i and y_i represent the characteristic line values of the i-th characteristic lines for the test samples and the modeling samples, respectively, while n represents the number of characteristic lines.

4. Results and discussion

4.1 Multi-model calibration marked with a single characteristic line

4.1.1 Correlation between characteristic line intensity and laser pulse energy. In this study, Fe II 261.18 nm was marked as the characteristic line reflecting the change in experimental conditions because it conforms to the selection basis of the above characteristic lines. To reveal the correlation between the intensity of the characteristic line and the laser pulse energy, this study systematically discusses the change trend of the intensity of the characteristic line under different laser pulse energies, as shown in Fig. 5. From the diagram, the linear fitting coefficient $R^2 = 0.992$ indicates a clear linear relationship between the intensity of the characteristic line and the laser pulse energy. When the laser pulse energy increases, the intensity of the characteristic line also increases; however, it can be observed that with the continuous increase of laser energy, the intensity of the characteristic line shows a certain fluctuation, which are caused by the instability of the laser output energy. Nevertheless, for the experimental parameters of 60 mJ laser pulse energy selected in this study, the fluctuation is small and has little effect on characteristic matching. Therefore, in general, the intensity of the characteristic line can still better reflect the change in laser pulse energy, providing a solid data

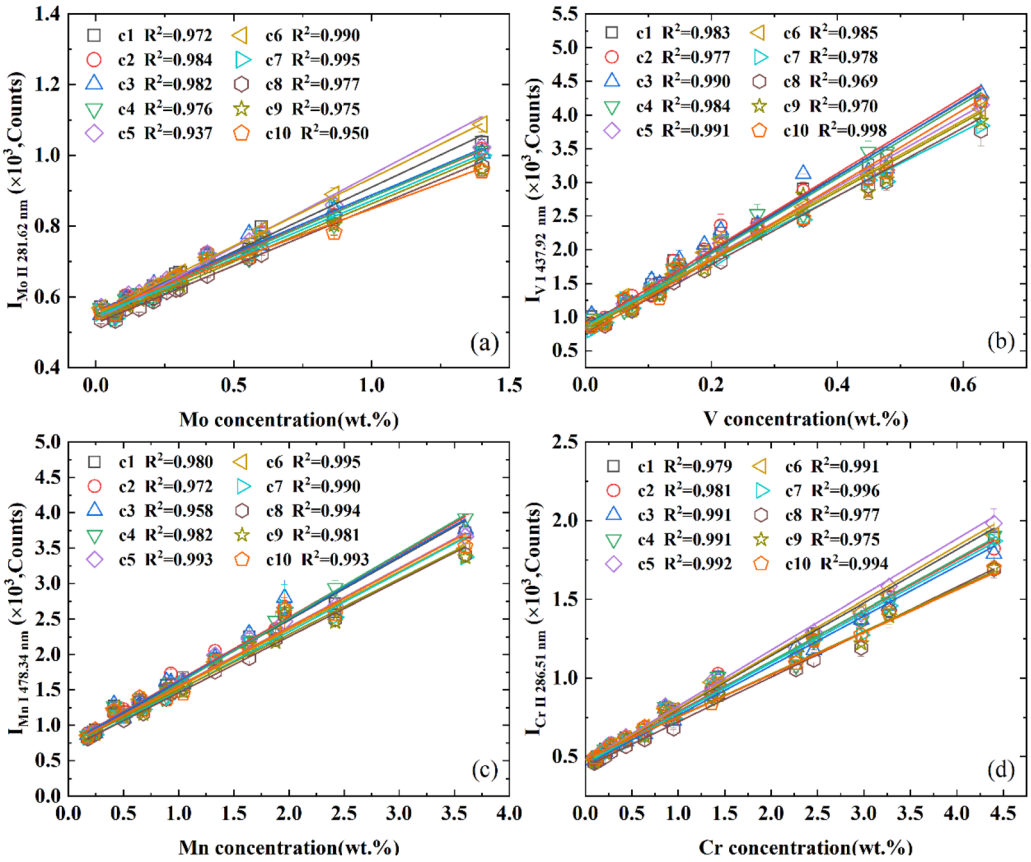

Fig. 4 Calibration models of four elements for ten consecutive days: (a) Mo; (b) V; (c) Mn; (d) Cr.

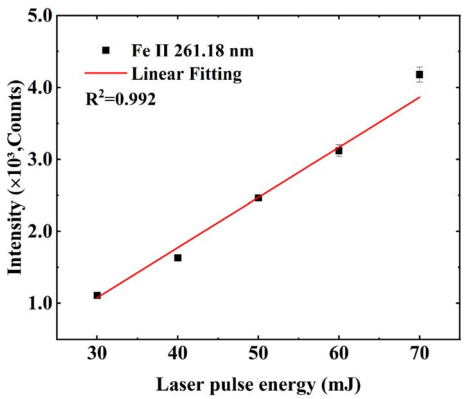

Fig. 5 Correlation between characteristic line intensity and laser pulse energy.

support for the characteristic line as the basis for reflecting the change in experimental conditions.

4.1.2 Characteristics extraction and matching. The spectral intensity of each modeling sample was extracted and calculated at the characteristic line Fe II 261.18 nm on the first day, and the average was taken as the characteristic line value (CL) for the calibration model of that day. The above process was repeated to calculate the respective characteristic line values for each of the 10 days (day 1–day 10). These values are presented in Table 2. As shown in Table 2, the CL values varied across different days, reflecting changes in experimental conditions over time. Although the variation in CL values was random, the fluctuation range remained limited, further demonstrating the feasibility of using the characteristic line. Similarly, the CL values of six test samples over five days (day 11–day 15) were extracted and calculated. The results are presented in Table 3.

When analyzing the test samples, the CL value of each test sample on the verification days is compared with the CL value of the calibration model for each corresponding period. According to eqn (1), the minimum CL deviation serves as the matching criterion to select the calibration model that corresponds to the calibration days, which is then used as the quantitative analysis model for the test sample. For instance, as shown in Table 3, the CL value of test sample 5 on day 11 was 3219.7 counts, which exhibited the smallest deviation from the CL value of 3219.9 counts recorded on day 2 in Table 2. Consequently, the calibration model from day 2 was employed for the quantitative analysis of test sample 5 on day 15. The quantitative analysis results for the four elements across all samples were compared with the standard values listed in Table 1, and the average relative errors were calculated to assess the accuracy of the quantitative analysis method. Additionally, the average standard deviations of the results for the four elemental contents in the test samples over five consecutive days were computed to

Table 2 The values of the characteristic line for calibration days (counts)

Day	1	2	3	4	5	6	7	8	9	10
CL	3230.4	3219.9	3052.3	3159.1	3355.7	3241.3	3060.6	3058.3	3145.3	3085.3

Table 3 The values of the characteristic line for verification days (counts)

Test sample no.	Day 11	Day 12	Day 13	Day 14	Day 15
5	3219.7	3242.9	3116.8	2753.0	2852.9
6	2844.8	2877.8	3029.8	2632.7	3037.1
9	2777.3	2924.7	2922.7	2763.3	2910.8
11	3210.6	3272.4	2962.7	2716.8	2940.4
16	3115.6	2970.1	2969.0	2824.6	2917.1
18	3065.8	3097.6	3377.4	2937.4	2940.6

evaluate the long-term reproducibility of the quantitative analysis method.

4.1.3 Improvement in accuracy. In the long-term verification of quantitative analysis methods, this study compared and evaluated the accuracy of the single calibration model (SM) method and the multi-model calibration marked with a single characteristic line (SCL-MM) method. As illustrated in Fig. 6, the average relative errors (AREs) of Mo, V, Mn, and Cr content prediction in six test samples based on the two methods over the five-day verification period are presented. Fig. 6(a)–(e) present the prediction results for test samples measured on days 11 to 15, respectively. Here, C1–C10 represent the single calibration model based on days 1–10, while T1–T5 represent the multi-calibration model marked with a single characteristic line. As demonstrated in the figure, C1 shows that the AREs of the five-day verification based on the calibration model of the first day are 8.9%, 9.2%, 11.2%, 18.9%, and 16.7%, with maximum daily fluctuation reaching 68.8% between days 13 and 14, and the error fluctuates greatly. Other AREs predicted based on a single calibration model (C2–C10) also vary from 8% to 19%, which indicates that there are significant differences in the performance of the single calibration model under different verification days, and the error fluctuation is obvious. This confirms the phenomenon reported in the literature, indicating that the change in experimental conditions has a great influence on the single calibration model, resulting in poor accuracy of its quantitative analysis results.[32]

In contrast, the AREs (T1–T5) obtained based on SCL-MM were 11.0%, 9.1%, 9.4%, 12.8%, and 11.4%, respectively. The overall fluctuation in error was significantly reduced, and the accuracy was also improved accordingly. For example, in Fig. 6(a), the ARE corresponding to model C8 is 18%. After applying the method proposed in this paper, T1 was reduced by 38.9% compared to C8, decreasing from 18% to 11%. Similarly, in Fig. 6(b), T2 decreased by 46.2% compared to C8, from 16.9% to 9.1%. The AREs obtained based on SCL-MM on other verification days also generally exhibit a downward trend, further demonstrating the effectiveness of the proposed method. Fig. 6(f) summarizes the five-day average results from Fig. 6(a)–(e). The results show that the average AREs based on the SM method are 13%, 13.2%, 11.5%, 12.4%, 13.2%, 13.3%, 12.3%, 13.4%, 12.5%, and 12.4%, respectively. The average ARE (TA) based on SCL-MM is 10.7%, which is lower than all the average AREs based on the SM method. Additionally, it is 13.0% lower than that of the optimal single model (C7) and 20.1% lower than that of the least effective single model (C8). These results demonstrate that the LIBS quantitative analysis method based on multi-model calibration marked with a single characteristic line can effectively solve the problem of error fluctuation caused by experimental condition drift and improve the accuracy of LIBS quantitative analysis after a long time interval.

4.1.4 Improvement in long-term reproducibility. To evaluate the improvement in long-term reproducibility of LIBS based on the SCL-MM method, Fig. 7 shows the average standard deviations (ASDs) of Mo, V, Mn, and Cr content predictions based on the SM method and the SCL-MM method over five days of verification. The SM method takes the C1 day calibration model as an example. The diagram illustrates that the ASD for the SCL-MM method is lower than that of the SM method. Specifically, for the Mn element, the ASD of the SCL-MM method is 21.4% lower than that of the SM method; for the Mo element, the ASD of the SCL-MM decreased by 10%; for the Cr element, the ASD of the SCL-MM decreased by 12.1%; and for the V element, the ASD decreased the most, by 34.6%. These results demonstrate that the method based on SCL-MM can effectively reduce the fluctuation of quantitative analysis results in long-term measurement and improve the long-term reproducibility of LIBS. This is because the change in the characteristic line intensity of the labeled matrix element Fe is mainly caused by the drift of the experimental parameters and changes in the environment. The SCL-MM method can compensate for changes in the experimental conditions by dynamically matching the characteristics and selecting the model closest to the current test conditions. For example, when the device parameters drift, the obtained LIBS data will also change. Substituting the established calibration model will cause the predicted value to deviate from the true value. The SCL-MM method matches the calibration model of the experimental conditions similar to the experimental conditions when the device parameters drift from many calibration models containing daily experimental condition information and corrects for the spectral intensity change caused by the device parameter drift, thereby maintaining the stability of the quantitative analysis results.

4.2 Multi-model calibration marked with multiple characteristic lines

Although the SCL-MM method improves the accuracy and long-term reproducibility of LIBS quantitative analysis to a certain

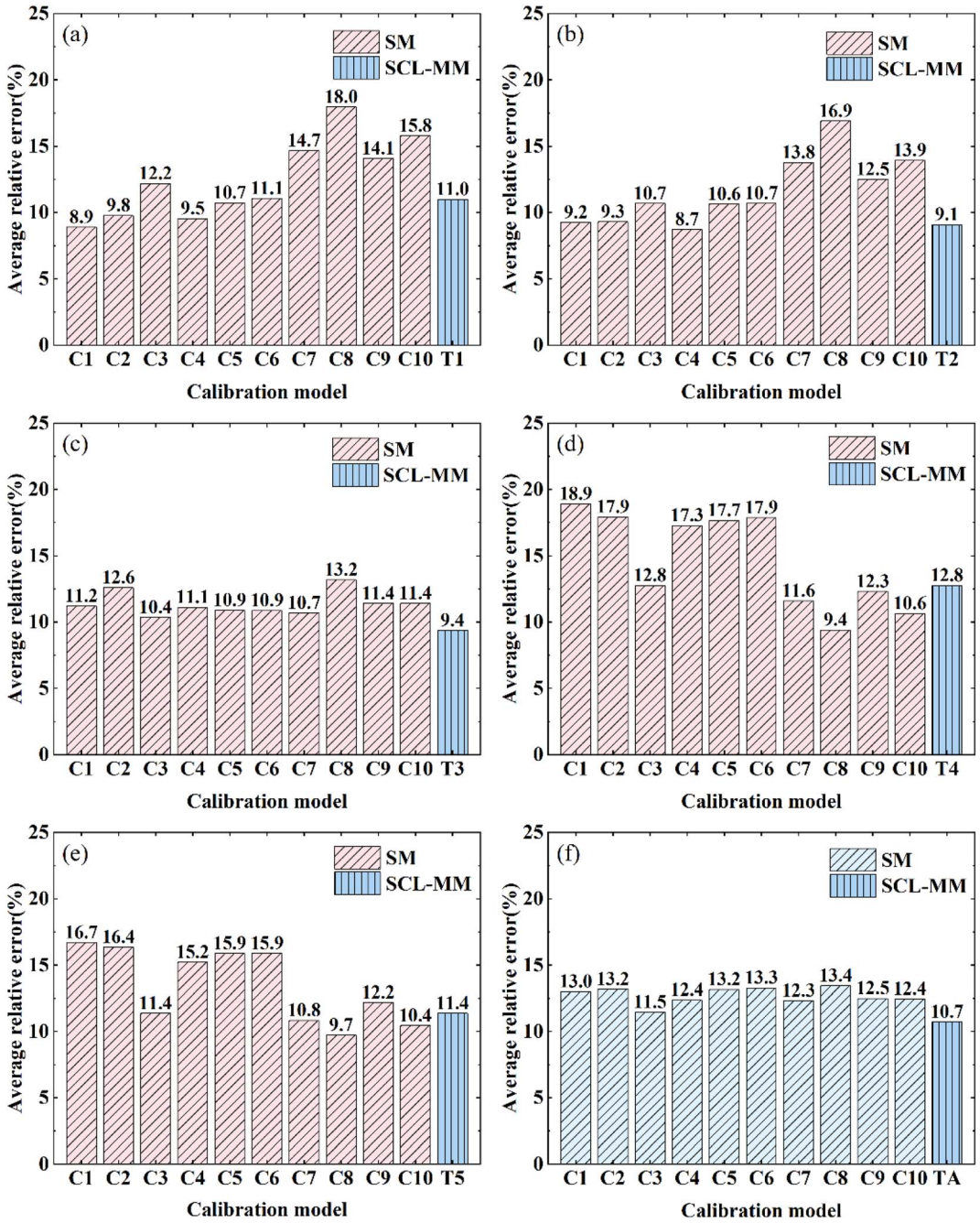

Fig. 6 Average relative errors (AREs) of Mn, Cr, Mo, and V element content prediction based on the SM method and the SCL-MM method: (a) day 11; (b) day 12; (c) day 13; (d) day 14; (e) day 15; (f) five-day average.

extent, it may still have the problem of incomplete reflection of experimental conditions. Because the single characteristic line only reflects the change of experimental conditions from one dimension, it may lead to inaccurate judgment of experimental conditions, which, in turn, affects the selection of calibration models and the accuracy of quantitative analysis results. To further optimize the model matching, this study proposes utilizing multiple characteristic line information as the characteristic matching model to improve the accuracy and rationality of the calibration model selection. In this research, three spectral lines (Fe II 234.81 nm, Fe II 261.18 nm, and Fe I 400.52 nm) were marked as characteristic lines to form multi-dimensional characteristics. The selection of these three characteristic lines not only meets the reference basis of the above characteristic lines but also distributes in different wavelength regions to enhance the anti-interference of environmental fluctuations and covers different ionization states to improve the compensation ability of the matrix effect. A three-dimensional characteristic vector $V_{\text{test}} = (I_{\text{FeII234.81}}, I_{\text{FeII261.18}}, I_{\text{FeI400.52}})$ is formed by the intensity of the three characteristic

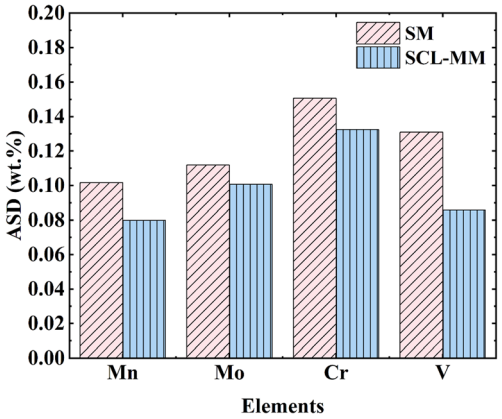

Fig. 7 Average standard deviations (ASDs) of Mo, V, Mn, and Cr content predictions based on the SM method and the SCL-MM method.

lines of the test sample on the verification date, and the Euclidean distance is calculated with the three-dimensional characteristic vector set $\{V_{cal}\}$ composed of the calibration model of each day. The Euclidean distance between each row of $\{V_{cal}\}$ (that is, the three-dimensional characteristic vector of each calibration model) and V_{test} is calculated respectively, and the calibration model with the smallest distance is selected as the best calibration model for quantitative analysis.

To confirm the validity of the method, this study compared the average relative errors (AREs) of the prediction of Mn, Cr, Mo, and V content in six test samples based on the multi-model calibration marked with a single characteristic line (SCL-MM) method and the multi-model calibration marked with multiple characteristic lines (MCL-MM) method. As shown in Fig. 8, the results indicate that, compared with the results obtained by the SCL-MM method, the ARE values for T1–T5 over five days using the MCL-MM method are 9.9%, 8.8%, 9.6%, 10.6%, and 9.5%, respectively. Except for the ARE value of T3, which increased slightly by 2%, the ARE values of the other four days decreased to a certain extent, among which T4 decreased by 17.2%, and the five-day average ARE value (TA) decreased by 9.35% compared with 10.7%. Although the MCL-MM method shows a limited increase in the AREs compared to the SCL-MM method, it effectively mitigates the influence of a single outlier by incorporating a comprehensive distance computation mechanism derived from multiple characteristic lines. This improvement can significantly enhance the robustness of model matching, thereby obtaining more stable and accurate quantitative analysis results.

In terms of long-term reproducibility, the method based on MCL-MM performs well. As illustrated in Fig. 9, the average standard deviations (ASDs) of the predicted values for the four elemental contents were presented based on the five-day verification period using the SM, SCL-MM, and MCL-MM methods. The SM utilizes the C1 calibration model as an example. The figure demonstrates that both SCL-MM and MCL-MM exhibit lower ASDs compared to SM. Specifically, for the elements Mn, Mo, Cr, and V, the ASD of SCL-MM decreased by 21.4%, 10%, 12.1%, and 34.6%, respectively, while the ASD of MCL-MM decreased by 33.3%, 32.3%, 41.2%, and 38.8%. These results indicate that the MCL-MM method is more effective in enhancing the long-term reproducibility of LIBS. The reason is that, compared with the single characteristic line, the multiple characteristic lines can reflect the change of experimental conditions more comprehensively and avoid the one-sidedness of the single characteristic line, allowing for a more accurate selection of the calibration model that closely matches the experimental conditions of the test data, which reduces measurement error and improves the long-term reproducibility of the quantitative analysis. It should be noted that although adding more characteristic lines may further improve the comprehensiveness of model matching, it may also introduce irrelevant or redundant information. This may lead to no significant change in the matching results, or even worse, increase the workload and complexity of data processing. In addition, the introduction of too many characteristic lines may also bring interference. For example, some characteristic lines may be interfered with by noise, resulting in large fluctuations

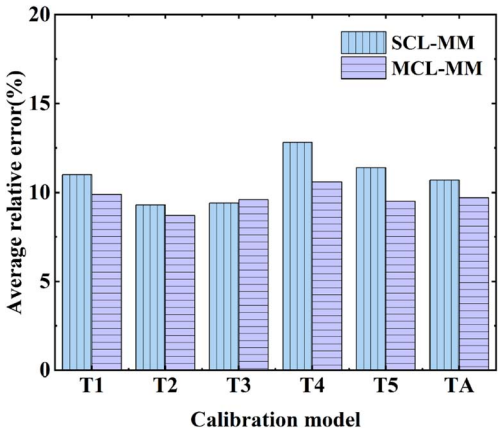

Fig. 8 Average relative errors (AREs) of Mn, Cr, Mo, and V element content prediction based on the SCL-MM method and the MCL-MM method.

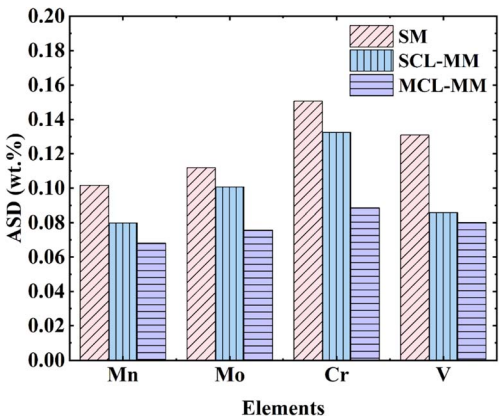

Fig. 9 Average standard deviations (ASDs) of the three quantitative analysis methods.

in values, thus affecting the stability of the matching results. The three characteristic lines selected in this paper have balanced performance and complexity. Future research will further explore the relationship between the number of characteristic lines and model matching, rather than simply pursuing an increase in the number.

5. Conclusion

This study proposes a LIBS quantitative analysis method based on multi-model calibration marked with characteristic lines, which effectively improves the accuracy and reproducibility of long-term LIBS measurements. Since experimental equipment parameters and environmental factors vary over time, multiple calibration models were established for different time periods to represent experimental conditions under various scenarios. Furthermore, characteristic line intensities that reflect changes in experimental conditions were used as characteristics to select the optimal calibration model for quantitative analysis. In this paper, using the analysis of Mo, V, Mn, and Cr elements in alloy steel as an example, calibration models were established over a 10 days period, and test samples were analyzed quantitatively over 5 days. The results showed that, compared to using a single calibration model, the proposed method significantly reduced both the AREs and the ASDs of the quantitative analysis results. This demonstrates that the long-term accuracy and reproducibility of LIBS quantitative analysis were improved. The proposed method provides a new quantitative analysis idea for LIBS technology, effectively addressing the issues of declining accuracy and reproducibility in calibration models over extended periods. Admittedly, the research in this paper is only a preliminary study on the feasibility of multi-model calibration marked with characteristic lines. More characteristic selection methods and multi-model establishment methods need to be further studied in subsequent studies.

Data availability

Raw data were generated at the laboratory facility. Part of the data has been embedded in the text as a chart, and other Derived data supporting the findings of this study are available from the corresponding author on request.

Conflicts of interest

There are no conflicts to declare.

Acknowledgements

This research was financially supported by the National Natural Science Foundation of China (No. 12464052, 12064029), Jiangxi Provincial Natural Science Foundation (No. 20242BAB25038) and Continuous-Support Basic Scientific Research Project (18BJ010261224900).

Notes and references

1 W. T. Li, X. Y. Li, X. Li, Z. Q. Hao, Y. F. Lu and X. Y. Zeng, *Appl. Spectrosc. Rev.*, 2020, **55**, 1–25.
2 L. M. Cabalín, T. Delgado, J. Ruiz, D. Mier and J. J. Laserna, *Spectrochim. Acta, Part B*, 2018, **146**, 93–100.
3 V. N. Lednev, P. A. Sdvizhenskii, R. D. Asyutin, R. S. Tretyakov, M. Y. Grishin, A. Y. Stavertiy, A. N. Fedorov and S. M. Pershin, *Opt. Express*, 2019, **27**, 4612–4628.
4 S. Legnaioli, B. Campanella, F. Poggialini, S. Pagnotta, M. A. Harith, Z. A. Abdel-Salam and V. Palleschi, *Anal. Methods*, 2020, **12**, 1014–1029.
5 K. Liu, C. He, C. W. Zhu, J. Chen, K. P. Zhan and X. Y. Li, *TrAC, Trends Anal. Chem.*, 2021, **143**, 116357.
6 Y. Zhang, T. L. Zhang and H. Li, *Spectrochim. Acta, Part B*, 2021, **181**, 106218.
7 N. H. Thomas, B. L. Ehlmann, D. E. Anderson, S. M. Clegg, O. Forni, S. Schröder, W. Rapin, P.-Y. Meslin, J. Lasue, D. M. Delapp, M. D. Dyar, O. Gasnault, R. C. Wiens and S. Maurice, *J. Geophys. Res.: Planets*, 2018, **123**, 1996–2021.
8 H. Saeidfirozeh, P. Kubelík, V. Laitl, A. Křivková, J. Vrábel, K. Rammelkamp, S. Schröder, I. B. Gornushkin, E. Képeš, J. Žabka, M. Ferus, P. Pořízka and J. Kaiser, *TrAC, Trends Anal. Chem.*, 2024, **181**, 117991.
9 J. Kaiser, K. Novotny, M. Z. Martin, A. Hrdlicka, R. Malina, M. Hartl, V. Adam and R. Kizek, *Surf. Sci. Rep.*, 2012, **67**, 233–243.
10 A. Velásquez-Ferrín, D. V. Babos, C. Marina-Montes and J. Anzano, *Appl. Spectrosc. Rev.*, 2021, **56**, 492–512.
11 Z. Hao, K. Liu, Q. Lian, W. Song, Z. Hou, R. Zhang, Q. Wang, C. Sun, X. Li and Z. Wang, *Front. Phys.*, 2024, **19**, 62501.
12 J. Liu, Z. Hou and Z. Wang, *J. Anal. At. Spectrom.*, 2023, **38**, 2571–2580.
13 R. Noll, C. Fricke-Begemann, M. Brunk, S. Connemann, C. Meinhardt, M. Scharun, V. Sturm, J. Makowe and C. Gehlen, *Spectrochim. Acta, Part B*, 2014, **93**, 41–51.
14 A. De Giacomo, M. Dell'Aglio, R. Gaudiuso, S. Amoruso and O. De Pascale, *Spectrochim. Acta, Part B*, 2012, **78**, 1–19.
15 G. Cristoforetti, M. Tiberi, A. Simonelli, P. Marsili and F. Giammanco, *Appl. Opt.*, 2012, **51**, B30–B41.
16 Y. Xu, Z. Hu, F. Chen, D. Zhang, J. Nie, W. Kou, W. Wang, F. Li and L. Guo, *J. Anal. At. Spectrom.*, 2022, **37**, 351–357.
17 G. Galbács, *Anal. Bioanal. Chem.*, 2015, **407**, 7537–7562.
18 U. Panne, C. Haisch, M. Clara and R. Niessner, *Spectrochim. Acta, Part B*, 1998, **53**, 1957–1968.
19 J. Feng, Z. Wang, Z. Li and W. Ni, *Spectrochim. Acta, Part B*, 2010, **65**, 549–556.
20 Z. Hao, L. Liu, M. Shen, R. Zhou, J. Li, L. Guo, X. Li, Y. Lu and X. Zeng, *J. Anal. At. Spectrom.*, 2018, **33**, 1564–1570.
21 Z. Hou, M. S. Afgan, S. Sheta, J. Liu and Z. Wang, *J. Anal. At. Spectrom.*, 2020, **35**, 1671–1677.
22 J. C. Liu, W. R. Song, W. L. Gu, Z. Y. Hou, K. K. Kou and Z. Wang, *Anal. Chim. Acta*, 2023, **1251**, 341004.
23 Z. Xu, L. Liu, Z. Hao, Z. Deng, Y. Lu, Z. Zhao, J. Li, J. Shi and X. He, *J. Anal. At. Spectrom.*, 2023, **38**, 2073–2079.

24 J. Nie, Y. Zeng, X. Niu, D. Zhang and L. Guo, *J. Anal. At. Spectrom.*, 2023, **38**, 2387–2395.
25 Y. Lu, L. Liu, Z. Wu, Z. Xu, Z. Zhao, Z. Hao, J. Shi and X. He, *J. Anal. At. Spectrom.*, 2023, **38**, 2619–2624.
26 N. Zhang, Z. Hao, L. Liu, B. Xu, S. Guo, X. Yuan, Z. Ouyang, L. Wang, J. Shi and X. He, *Talanta*, 2025, **284**, 127232.
27 Z. Yu, S. Yao, L. Zhang, Z. Lu, Z. S. Lie and J. Lu, *J. Anal. At. Spectrom.*, 2019, **34**, 172–179.
28 A. L. Krüger, G. Nicolodelli, P. R. Villas-Boas, A. Watanabe and D. M. B. P. Milori, *Plasma Chem. Plasma Process.*, 2020, **40**, 1417–1427.
29 J. Thomas and H. Joshi, *Appl. Spectrosc. Rev.*, 2023, **59**, 124–155.
30 D. W. Hahn and N. Omenetto, *Appl. Spectrosc.*, 2012, **66**, 347–419.
31 Q. Zhong, T. Zhao, X. Li, S. Nie, H. Xiao, Y. Ma, W. Cheng, G. Guo and Z. Fan, *Opt. Lett.*, 2021, **46**, 5244–5247.
32 Y. Zhou, L. Sun, Y. Li, Y. Xin, W. Dong and J. Wang, *J. Anal. At. Spectrom.*, 2024, **39**, 1778–1788.